3.16 THERMAL NOISE

Thermal noise refers to electromagnetic interference generated by power supplies, transformers, transmission cables, and other electronic components. Characterizations of thermal noise in simulations are difficult due to the unknown nature of the relative contributions of the various factors, but noise figures are routinely derived from system measurements. Shielding, component physical layout, and equipment condition also affect noise levels to varying degrees. An area of interest is the treatment of thermal noise in the model and its effect on signal processing, target detection, and tracking performance.

Data Items Required

Data Item		Accuracy	Sample Rate	Comments
4.1.1	Noise power	±0.1 dB	SV/T	
4.1.2	Detection time	±0.5 s	SV/T	
4.1.3	Tracking azimuth	±0.1 deg	10 Hz	
4.1.4	Tracking elevation	±0.1 deg	10 Hz	
4.1.5	Tracking range	±5 m	10 Hz	
4.1.6	Receiver noise figure	±1 dB	1 dB steps	
4.1.7	Noise bandwidth	±0.1 dB	SV/T	
4.1.8	Target echo	±0.5 dB	10 Hz	

3.16.1 Objectives and Procedures

RADGUNS uses constants to represent noise levels in the acquisition and tracking radars, which, for some systems, are one in the same. Signal threshold for target detection is sensitive to variations in PNOISA (Parametric Noise - Acquisition) values because they contribute to the denominator in the signal-to-noise (S/N) ratio used to establish a detectable signal level. PNOIST (Parametric Noise - Tracking) values affect the ability of the tracking radar to maintain S/N levels necessary for continuation of autotrack. High noise levels could result in break locks if the target signature fades suddenly, or a lower than normal jammer power could prevent establishment of autotrack for a given target RCS.

The method for examining acquisition sensitivity of the thermal noise function was to exercise *RADGUNS* for the following conditions:

a. Model mode: DETR
b. Target RCS: 1.0 m^2
c. Target altitude: 200 m (clutter disabled)
d. Flight path: LINEAR
e. Radar type: RAD1
f. PNOISA: 0.5, 1.0, 1.5, and 2.0 nominal
g. Output: S/N ratio and detection range

Tracking errors in angle and range are sensitive to variations in the PNOIST value.

RADGUNS was exercised using the following conditions:

a. Model mode: SNGL/RADR
b. Target RCS: 10 dBsm
c. Target altitudes: 500 m
d. Flight path: LINEAR
e. Radar type: RAD1
f. PNOIST: 0.5, nominal, 2.0
g. Output: Azimuth, elevation, and range tracking errors

3.16.2 Results

Two linear flight paths were selected to analyze thermal noise tracking error sensitivity: a zero-offset (to stress elevation tracking) and a 1000-m offset (to stress azimuth tracking). Both targets were flown at the same velocity (200 m/s). A 10-m^2 TPA target was flown with MTI off, clutter and multipath disabled. Using three different PNOIST values (nominal, 0.5 x nominal, and 2.0 x nominal), six simulation runs were executed to examine angle and range tracking errors. Variances in mean, standard deviation, characteristic frequency, and RMS were used to gauge sensitivity to changes in thermal noise.

Figure 3.16-1 shows the sensitivity of detection range to a variance in parametric noise (PNOISA). The information shown is summarized in Table 3.16-1. For a ±10% variance in PNOISA value, detection range varies less than ±500 m and S/N ratio varies less than ±10%. Larger and smaller target RCS values would shift the curve to the right or left.

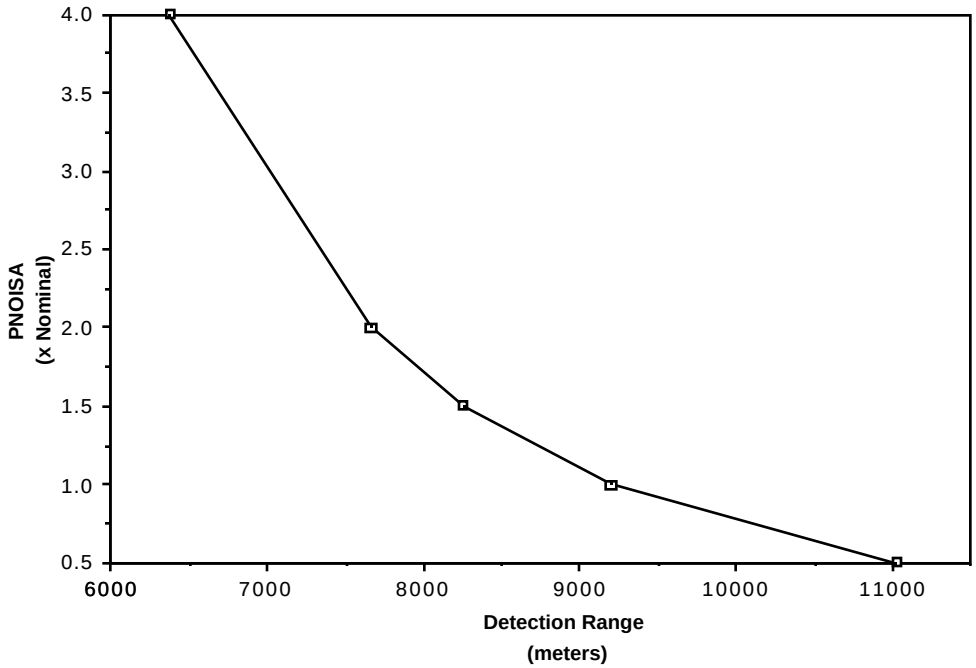

FIGURE 3.16-1. Detection Range as a Function of Parametric Noise (PNOISA).

TABLE 3.16-1. Detection Range and S/N Ratio Variance as a Function of Parametric Noise (PNOISA).

PNOISA Value	Detection Range (m)	S/N
0.5 x Nominal	11022	25.17
Nominal	9192	25.22
1.5 x Nominal	8262	25.22
2.0 x Nominal	7663	25.16
4.0 x Nominal	6373	25.14

Figure 3.16-2 depicts azimuth errors for the three 1000-m offset cases. Note that detection, as previously discussed, appears to function properly, with higher noise levels producing later detections. The three engagements each span a 200-s time period, with crossover (in range) occurring at 100 s. Although the three curves show marked differences in the fringe regions, within the zone of primary interest (8000 m, or between 60 and 140 s) the curves display strong similarities. It can be seen in the figure that four distinct patterns characterize azimuth tracking error response:

a. Long-range ingress (time 0 to approximately 60 s), where acquisition occurs, frequency response is low and means for all three curves are close to zero.

b. Short-range ingress (time 60 to 100 s), where frequency response is faster, means move sharply to positive values, and the target enters effective gun range.

c. Short-range egress (time 100 to approximately 140 s), characterized by a frequency response similar to short range ingress, but with negative mean values; the target flies out of effective gun range in this zone.

d. Long-range egress (time 140 to 200 s), in which the low and nominal noise cases show a frequency response, the high noise case appears unstable, and the means again approach zero.

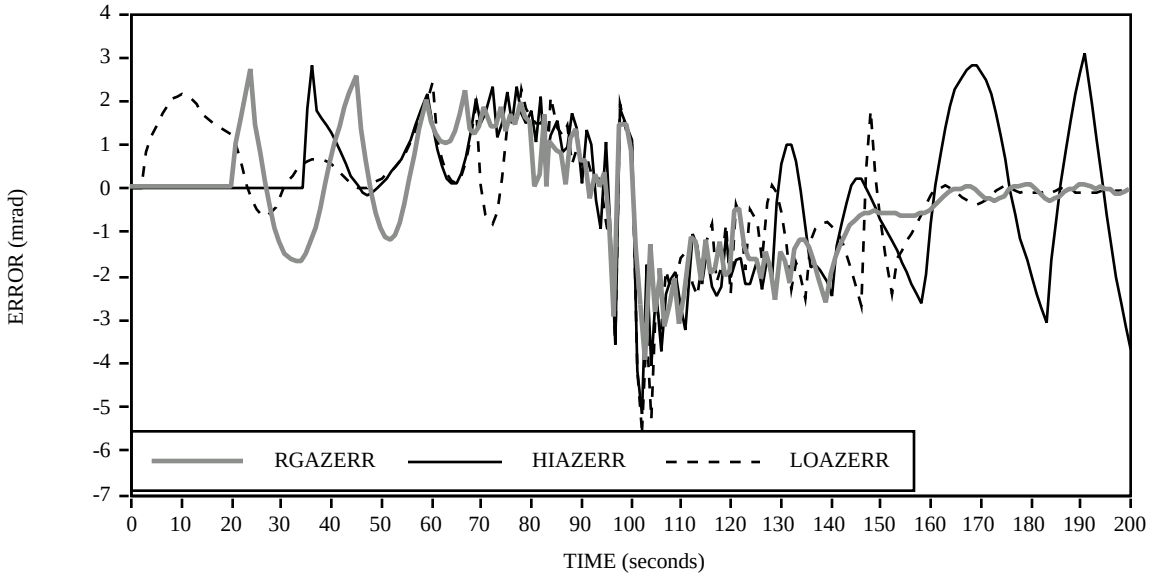

FIGURE 3.16-2. Azimuth Error Comparison for the 1000-Meter Offset Runs.

Based upon this graphical analysis, it was determined that detailed statistical calculations of sensitivity would be made for the short-range cases only. The reasons for this decision were: (a) only the short-range zones are within effective gun range, and (b) the effects of noise changes on azimuth tracking errors for the long-range zones is obvious from the figure. To bound the analysis among all six runs, common ingress and egress zones were selected which: (a) avoided crossover (where large tracking errors would unnecessarily bias the overall results), (b) would not include any time period not in autotrack (such as prior to detection, out of range and receding, or during break lock and reacquisition, and (c) would be equal in duration. The zones which met these specifications were ingress from time 66 to 99 s and egress from 104 to 137 s. These zones will be referred to as ingress and egress, respectively, in the remainder of this section for each run analysis.

Returning to the 1000-m offset, azimuth tracking error comparison, Table 3.16-2 lists the key statistical parameters and the percentage of variance for ingress. The symbols in the table represent mean ($\bar{X}$), standard deviation (σ), average ingress frequency (f_i), and root-mean-square (RMS) error values. The data suggests that for azimuth tracking error, large thermal noise changes resulted in relatively small percentage changes in all four parameters. The more significant issue apparent in the data is the extremely small magnitude of change in mean and standard deviation (< 0.2 mrad). RMS error magnitude for the high noise case is only 1.54 mrad.

TABLE 3.16-2. 1000-Meter Offset Ingress Azimuth Tracking Error Comparison.

Parameter	Nominal	High Noise (Nom x 2.0)	% Change	Low Noise (Nom x 0.5)	% Change
$\bar{X}$ *	0.90	1.05	+16.3	0.72	–20.1
σ *	0.98	1.14	+16.8	1.18	+20.4
f_i **	0.23	0.29	+25.0	0.23	0.0
RMS *	1.32	1.54	+16.6	1.36	+3.5

* – Values in mrad.
** – Values in Hz.

Table 3.16-3 contains parametric data comparisons for the egress portion of these runs (f_e represents average egress frequency). The most significant parametric variance was standard deviation, which showed high induced instability with either increasing or decreasing thermal noise. The magnitude of these variances, however, is less than 0.7 mrad.

TABLE 3.16-3. 1000-Meter Offset Egress Azimuth Tracking Error Comparison.

Parameter	Nominal	High Noise (Nom x 2.0)	% Change	Low Noise (Nom x 0.5)	% Change
$\bar{X}$ *	–1.78	-1.68	+5.2	-1.65	+7.1
σ *	0.63	1.24	+96.4	1.07	+69.8
f_e**	0.26	0.23	-11.1	0.23	-11.1
RMS *	1.88	2.08	+10.5	1.96	+4.1

* – Values in mrad.
** – Values in Hz.

Figure 3.16-3 illustrates elevation tracking errors for the zero-offset runs and Table 3.16-4 contains ingress parametric data for zero-offset elevation errors. Although the variances are again very small in magnitude, it is interesting to note that increasing noise reduced elevation tracking errors; moreover, decreasing noise resulted in increased errors. The large frequency change percentages are visible in Figure 3.16-3.

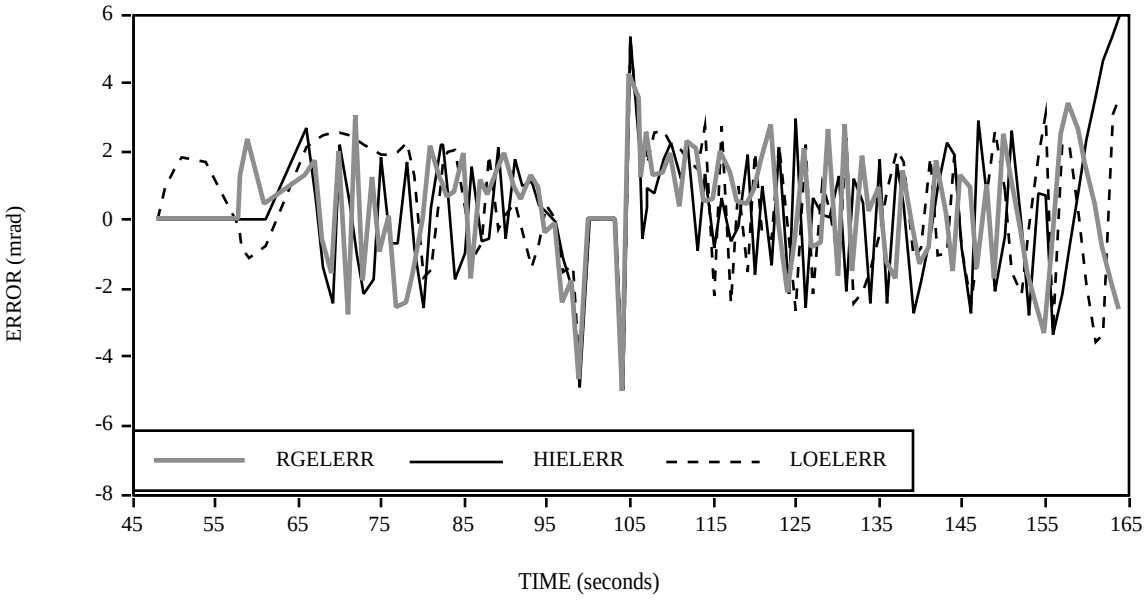

FIGURE 3.16-3. Elevation Error Comparison for the Zero Offset Runs.

TABLE 3.16-4. Zero Offset Ingress Elevation Tracking Error Comparison.

Parameter	Nominal	High Noise (Nom x 2.0)	% Change	Low Noise (Nom x 0.5)	% Change
$\bar{X}$ *	0.14	0.06	–57.7	0.88	+511.2
σ *	1.59	1.52	–4.0	1.46	–8.1
f_i **	0.30	0.24	–20.0	0.18	–40.0
RMS *	1.74	1.70	–2.3	1.82	+5.0

* – Values in mrad.
** – Values in Hz.

The egress data are presented in Table 3.16-5. Note again the reduction of error (mean and RMS) with an increase in noise, albeit of very small magnitude. Standard deviations for both an increase and a decrease in noise rose slightly, while RMS for the low-noise case actually increased.

TABLE 3.16-5. Zero Offset Egress Elevation Tracking Error Comparison.

Parameter	Nominal	High Noise (Nom x 2.0)	% Change	Low Noise (Nom x 0.5)	% Change
$\bar{X}$ *	0.79	0.32	–59.4	0.55	-30.1
σ *	1.85	1.94	+5.2	2.18	+17.7
f_e **	0.33	0.45	+36.4	0.36	+9.1
RMS *	1.99	1.94	–2.1	2.25	+13.1

* – Values in mrad.
** – Values in Hz.

Range tracking error is less affected by changes in thermal noise than either azimuth or elevation. Figure 3.16-4 depicts range errors for the 1000-m offset cases. It is readily apparent from the figure that the three sets of data are very similar in both frequency and amplitude. Correlation coefficients for these cases are well above 0.9. The pertinent ingress statistics for these runs are listed in Table 3.16-6. Small percentages of change and even smaller magnitude values render range tracking error virtually insensitive to changes in thermal noise.

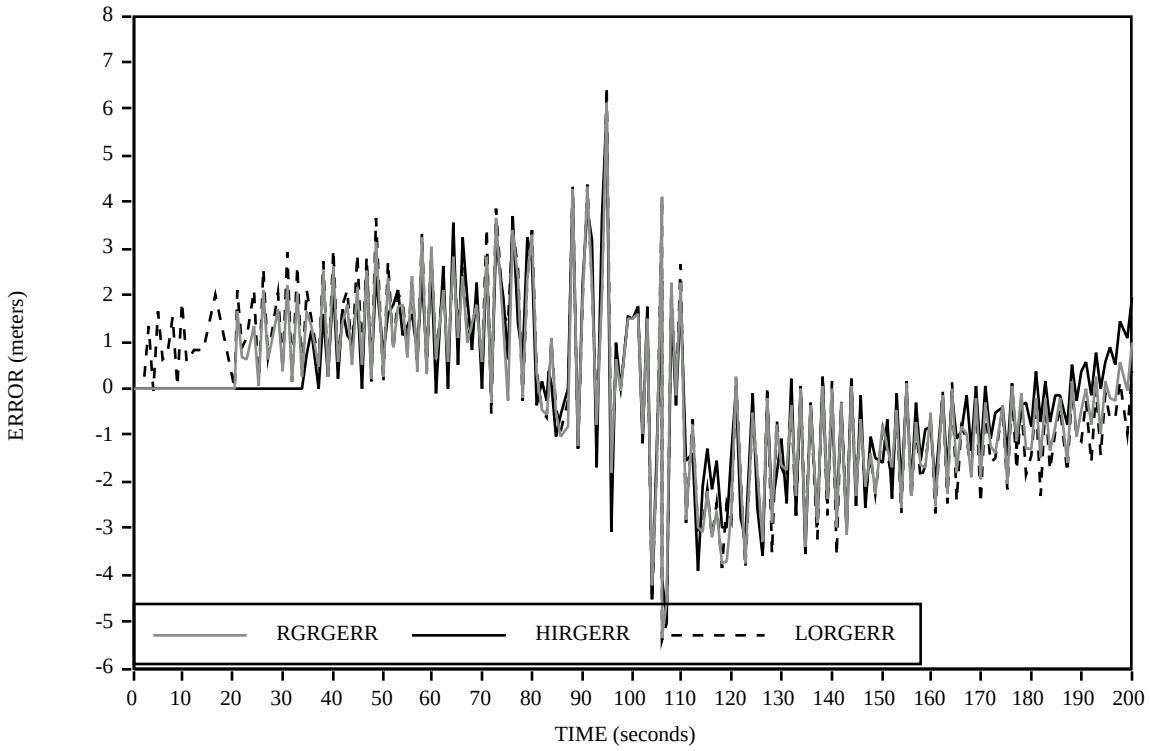

FIGURE 3.16-4. Range Error Comparison for the 1000-Meter Offset Runs.

TABLE 3.16-6. 1000-Meter Offset Ingress Range Tracking Error Comparison.

Parameter	Nominal	High Noise (Nom x 2.0)	% Change	Low Noise (Nom x 0.5)	% Change
$\bar{X}$ *	1.22	1.32	+8.7	1.35	+10.7
σ *	1.85	1.96	+6.4	1.89	+2.2
f_i **	0.33	0.39	+18.2	0.36	+9.1
RMS *	2.19	2.34	+7.1	2.30	+4.9

* – Values in mrad.
** – Values in Hz.

The egress statistics for these runs are listed in Table 3.16-7. Again, the insensitivity of range tracking errors to changes in noise is apparent.

TABLE 3.16-7. 1000-Meter Offset Egress Range Tracking Error Comparison.

Parameter	Nominal	High Noise (Nom x 2.0)	% Change	Low Noise (Nom x 0.5)	% Change
$\bar{X}$ *	–1.81	–1.73	+4.2	–1.82	-0.6
σ *	2.04	1.78	–12.5	2.11	+3.3
f_i **	0.39	0.36	–7.7	0.42	+7.7
RMS *	2.70	2.47	–8.7	2.76	+2.1

* – Values in mrad.
** – Values in Hz.

Figure 3.16-5 illustrates the zero-offset runs. This data correlates with coefficient values above 0.9. As in the two previous zero-offset cases, graphical editing was used to enhance readability.

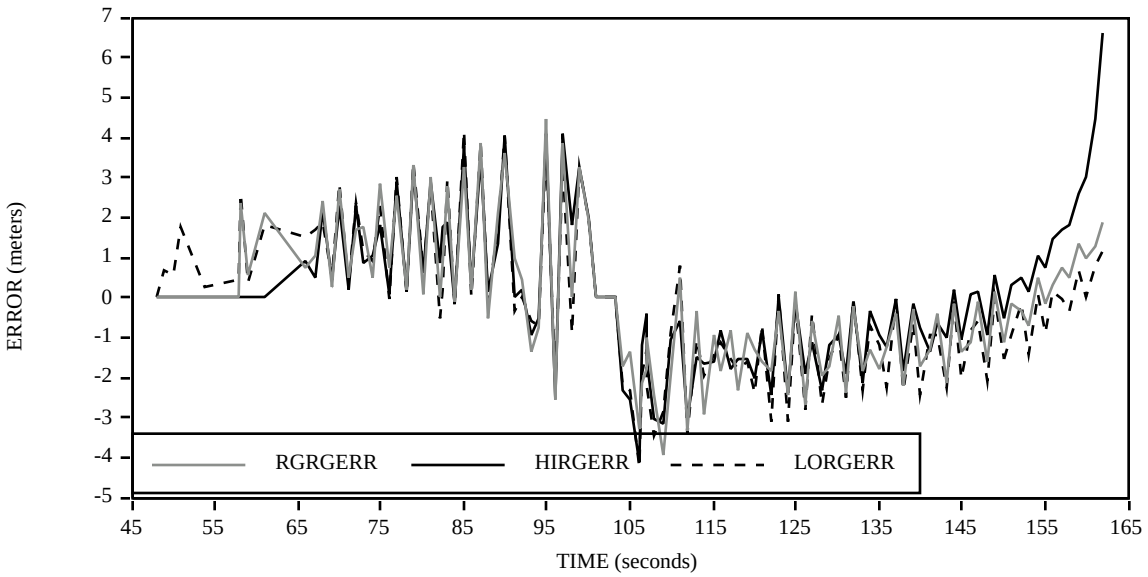

FIGURE 3.16-5. Range Error Comparison for the Zero-Offset Runs.

Tables 3.16-8 and 3.16-9 list the pertinent statistical parameters associated with ingress and egress, respectively.

TABLE 3.16-8. Zero Offset Ingress Range Tracking Error Comparison.

Parameter	Nominal	High Noise (Nom x 2.0)	% Change	Low Noise (Nom x 0.5)	% Change
$\bar{X}$ *	1.39	1.40	+0.9	1.35	-3.1
σ *	1.68	1.60	-4.9	1.70	+1.2
f_i **	0.39	0.42	+7.7	0.42	+7.7
RMS *	2.16	2.11	-2.5	2.15	-0.6

* – Values in mrad.
** – Values in Hz.

TABLE 3.16-9. Zero Offset Egress Range Tracking Error Comparison.

Parameter	Nominal	High Noise (Nom x 2.0)	% Change	Low Noise (Nom x 0.5)	% Change
$\bar{X}$ *	-1.58	-1.54	+2.5	–1.70	–7.8
σ *	1.01	0.98	–3.6	1.15	+13.7
f_e **	0.39	0.36	–7.7	0.36	-7.7
RMS *	1.87	1.82	–2.8	2.05	+9.5

* – Values in mrad.
** – Values in Hz.

3.16.3 Conclusions

Detection range is sensitive to changes in the PNOISA value. A 50% reduction in PNOISA produces an increase in detection range of 1830 m, while a 50% increase in PNOISA produces a decrease in detection range of 930 m. A detection range accuracy equivalent to the minimum resolution due to target speed and detection time (±1 s), or a few tens of meters, should be used in comparisons with model predictions. Noise power and bandwidth measurements are usually reported to B accuracy, which should be sufficient for assessment of this functional element.

Analysis has indicated that changes in thermal noise yield noticeable changes in the pattern and amplitude of azimuth and elevation angle tracking errors. However, the magnitudes of these changes are so small as to render them insignificant. Table 3.16-10 lists the average and maximum parameter values for the 100% noise increase runs. Note that the extremely small values are perhaps below the resolution limits of current range tracking equipment. Note also, that range tracking is virtually insensitive to the noise increases.

TABLE 3.16-10. Parameter Magnitudes for 100% Noise Increase.

	$\bar{X}$ Avg	σ Avg	RMS Avg
Azimuth Tracking Error	0.12 mrad (0.19 mrad max)	0.30 mrad (0.61 mrad max)	0.22 mrad (0.44 mrad max)
Elevation Tracking Error	0.23 mrad (0.47 mrad max)	0.08 mrad (0.17 mrad max)	0.09 mrad (0.26 mrad max)
Range Tracking Error	0.06 m (0.11 m max)	0.12 m (0.26 m max)	0.12 m (0.24 m max)

Table 3.16-11 contains the same data for the 50% noise reduction runs.

TABLE 3.16-11. Parameter Magnitudes for 50% Noise Reduction.

	$\bar{X}$ **Avg**	σ **Avg**	**RMS Avg**
Azimuth Tracking Error	0.14 mrad (0.21 mrad max)	0.22 mrad (0.44 mrad max)	0.10 mrad (0.25 mrad max)
Elevation Tracking Error	0.37 mrad (0.74 mrad max)	0.13 mrad (0.33 mrad max)	0.14 mrad (0.26 mrad max)
Range Tracking Error	0.08 m (0.13 m max)	0.07 m (0.14 m max)	0.09 m (0.18 m max)

Changes in thermal noise produced noticeable changes in frequency response for the angle tracking channels. When considering the extremely small amplitudes involved, however, the changes in frequency will probably not affect overall gun system performance.